

Full Length Research Paper

Generation of land cover map using geospatial tools: A case study from Ardebil, Iran

Ehsan Sahebjalal* and Ahmad Heidari

Soil Science Department; Faculty of Agricultural Engineering and Technology, University College of Agriculture and Natural Resources, University of Tehran, Iran.

Accepted 23 August, 2011

Remote sensing and geographical information system (GIS) have gained importance as powerful and efficient tools for land cover mapping. Digital image classification is generally performed to produce land cover maps from remote sensing data, particularly for large areas. In this study, IRS LISS III data was prepared for producing land cover map of study area, Ardebil, Iran. Digital image processing techniques were conducted for the processes of radiometric and geometric correction and classification for land cover analysis. Digital elevation model (DEM) was performed by digitizing 1/50000 scaled standard topographic map. Slope map were derived by using the DEM as layers in GIS and overlain on the classified image to delineate land cover classes including slope limits of study area for subsequent applications such as land use planning. According to results, the produced land cover map had an overall accuracy equal to 80% indicating an acceptable accuracy for this classification.

Key words: Land cover, geographical information system (GIS), remote sensing, confusion matrix, image processing, supervised classification.

INTRODUCTION

The knowledge of spatial land cover information is essential for proper management, planning and monitoring of natural resources (Zhu, 1997). For example, it is a desired input for many agricultural, geological, hydrological, and ecological models. Also, any natural disaster study such as landslide hazard zonation (Gupta et al., 1999; Saha et al., 2002) highly depends on the availability of accurate and up-to-date land cover information. Remote sensing technique has ability to represent various land cover categories by means of classification process. Geographical information systems have the ability to interrelate spatially multiple types of information assembled from different sources. Satellite remote sensing, in conjunction with geographic information systems, has been widely applied and recognized as a powerful and effective tool in analyzing land cover/use categories (Ehlers et al., 1990; Harris and Ventura, 1995; Weng, 2001). In this study, the LISS III image (23.5 m spatial resolution) has been used as the

primary data to produce land cover map using supervised classification. Supervised classification is the process of using training samples, samples of known identity to classify pixels of unknown identity. The supervised classification is generally followed by knowledge-based expert classification systems depending on reference maps to improve the accuracy of the classification process (Berberoglu et al., 2007; Xiaoling et al., 2006). We can add ancillary data such as slope, to the land cover map for regional planning. Besides, the classification of land use/cover types provides useful information in mapping vegetation and ecosystem types (Hirataa et al., 2001; Vieira et al., 2003; Zhu, 1997). Then, these thematic maps can be also used to generate necessary database for empirical and process-based models of soil loss, hydrological cycle, and carbon flux (Anderson et al., 2006; Shi et al., 2007; De Jong, 1999; Evrendilek et al., 2007).

Current land use and land cover data are needed by planners, managers and decision makers to investigate the land cover distribution and existing activities on lands. To produce land cover maps, relating data must be collected from different resources such as aerial photographs

*Corresponding author. E-mail: e.sahebjalal@gmail.com.

and satellite imageries. Since using satellite imageries can reduce the time and cost of collecting and analyzing data, it turns into the most common tool for this purpose. This study made use of remotely sensed data and GIS technologies to generate land cover map of a study area in the province of Ardebil, Iran, and investigate the accuracy of produced map.

STUDY AREA

Location of the study area is given in Figure 1. The study area of about 3391.54 ha is situated between 38°17' to 38°21' N and 48°27' to 48°33' E in Ardebil, Iran. The physiographic map of the study area presents more or less a flat land with no hills or forests. Mean annual temperature of the study area fluctuates between 7.9 and 15.2°C and its mean annual precipitation is 333.9 mm. This area has an altitude ranging from approximately 1300 to 1340 m above sea level. The main soil type met with in this area is vertisol and the soil moisture and temperature regimes are dry xeric and mesic, respectively. Most of the area is covered by grassland and range but also a significant extent is under cultivation (rainfed and irrigated) and the agricultural products includes a variety of wheat, barley, cotton and potatoes.

METHODOLOGY

The present study is based on mapping land cover from IRS-1C remote sensing data. The image was acquired in 25th October, 2002 in path 66 and row 43. A number of data processing steps are involved in performing image classification. These include preprocessing of LISS III image to correct for atmospheric errors, geometric correction of image, image classification and accuracy assessment. All the processing has been done on Arc GIS and ILWIS software. In the following, the processing steps are briefly described.

Pre-processing of LISS III image

The atmospheric scattering is common in remote sensing data and is generally more pronounced in the shorter wavelength regions (e.g., blue). The effect of atmospheric scattering is to contribute some additional spectral values to the ground reflectance (Gupta, 2003; Jensen, 1986). In this study, the LISS III image was corrected for atmospheric path radiance using dark object subtraction method (Chavez, 1988). The method is fast and easy, as it does not require information on atmospheric conditions at the time of image acquisition. To implement this method, the pixel (associated with the dark object) having minimum brightness value in the near infra red (NIR) band was detected and the corresponding pixel values in all other bands were subtracted from the specific raw bands. This will result in an image that is corrected for atmospheric scattering.

Geometric correction of image

To locate ground features on imagery, or to compare a series of images, a geometric correction procedure is used to register each pixel to real world coordinates (Jensen, 1996). Accurate geometric

registration of images is a pre-requisite to perform image classification. The LISS III image was geometrically corrected using 20 well-distributed ground control points (GCPs) extracted from the 1/50000 scaled topographical map on Arc GIS software by using first order polynomial and nearest neighbor resampling method. Total root mean square (RMS) error was 0.49 pixels (11.5 m) for this image.

Image classification

A series of image classification operations were performed to produce land cover map from LISS III image. At first using field survey data, training sets for classification were prepared on ILWIS software and used as reference data to generate ground truth map. Then the image was classified using maximum likelihood method and land cover map was produced. At the last stage of image processing, calculation of accuracy assessment of classification was performed. Accuracy assessment is an important feature of land-cover and land-use mapping, not only as a guide to map quality and reliability, but also in understanding thematic uncertainty and its likely implications to the end user. The classification accuracy in remote sensing shows the correspondence between a class label allocated to pixel and true class. The true class can be observed in the field, either directly or indirectly from a reference map (Janssen and Vander, 1994). To determine the accuracy of classification, produced land cover map and ground truth map was compared. The pixels of agreement and disagreement are generally compiled in the form of a confusion matrix. It is a $c \times c$ matrix (c is the number of classes), the elements of which indicate the number of pixels in the testing data. The columns of the matrix depict the number of pixels per class for the classified image, and the rows show the number of pixels per class for the reference data. From this confusion matrix, a number of accuracy measures such as overall accuracy, average accuracy and average reliability may be determined. The overall accuracy is used to indicate the accuracy of whole classification (that is, number of correctly classified pixels divided by the total number of pixels in the error matrix). Average accuracy is the sum of class's accuracy divided by the number of classes. Average reliability represents the number of pixels on reference data that have been correctly classified divided by whole pixels that is classified as those classes.

RESULTS AND DISCUSSION

The aim of this study is to implement an image classification approach to produce an accurate land cover map for its subsequent use in GIS based application on agricultural uses such as land suitability assessment. After image pre-processing, using different parameters such as correlation matrix and creating several false color composites, the best color composite with the highest radiometric resolution were determined (FCC 321) for LISS III image. Then using training sets, the image was classified. Land cover map was produced and crossed with ground truth maps. Table 1 shows the correlation matrix of LISS III image. Figure 2 shows the classified image.

The result of digital satellite image classification is a pixel by pixel labeling of the entire image. Raster data converted to vector layer for presentation and analysis in Arc GIS software. In order to show majority of the classes, many small polygons which have less than 5 ha

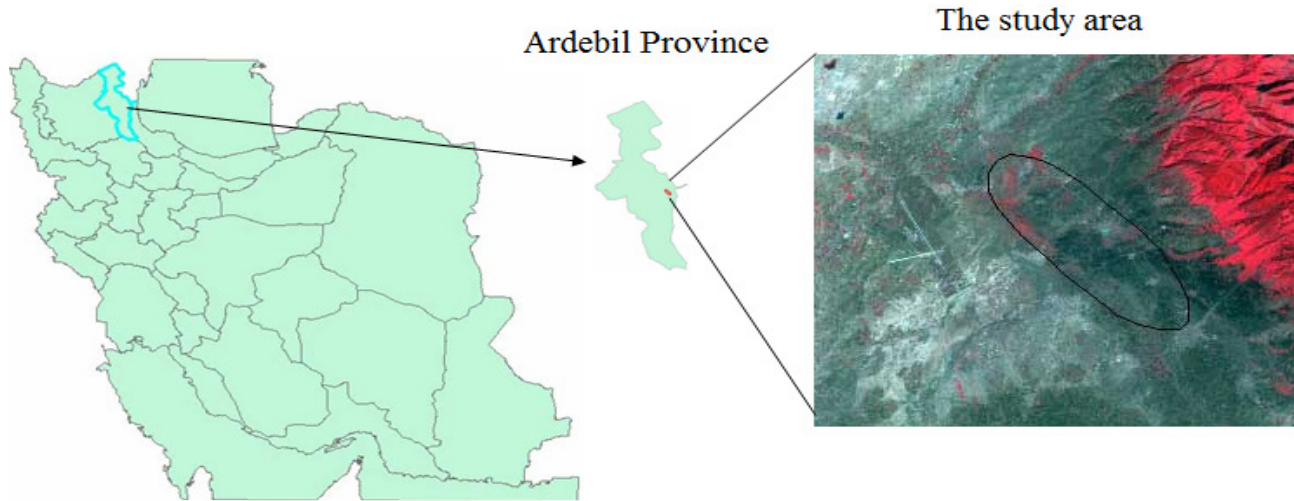


Figure 1. Location of the study area showed on the IRS LISS III image, Ardebil, Iran.

Table 1. Correlation matrix of LISS III image.

Bands	Band 1	Band 2	Band 3
Band 1	1	0.98	0.98
Band 2	0.98	1	1
Band 3	0.98	1	1

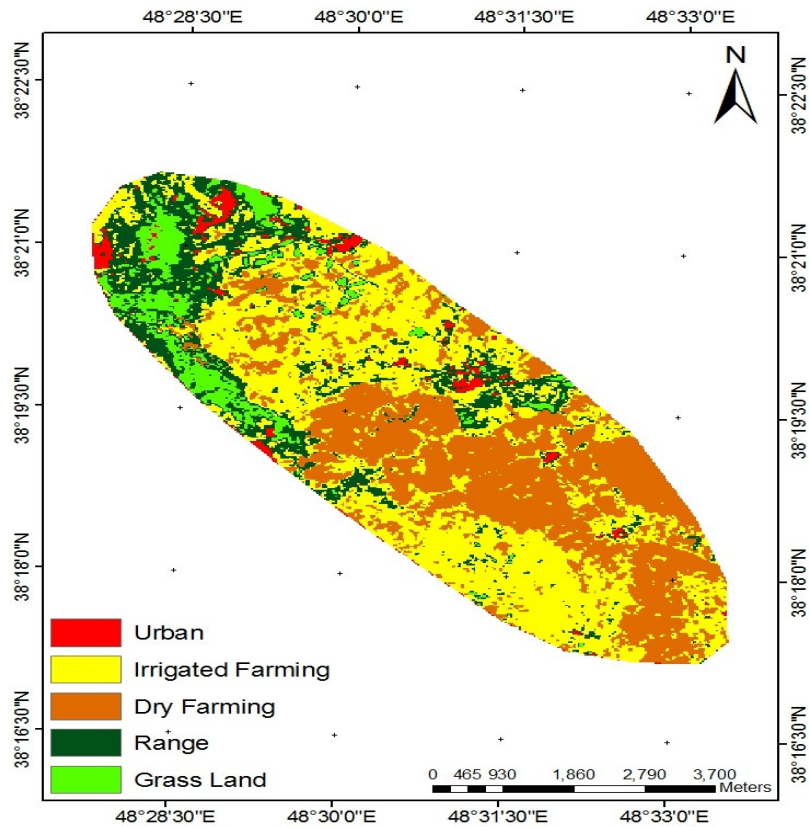


Figure 2. Classified image of study area.

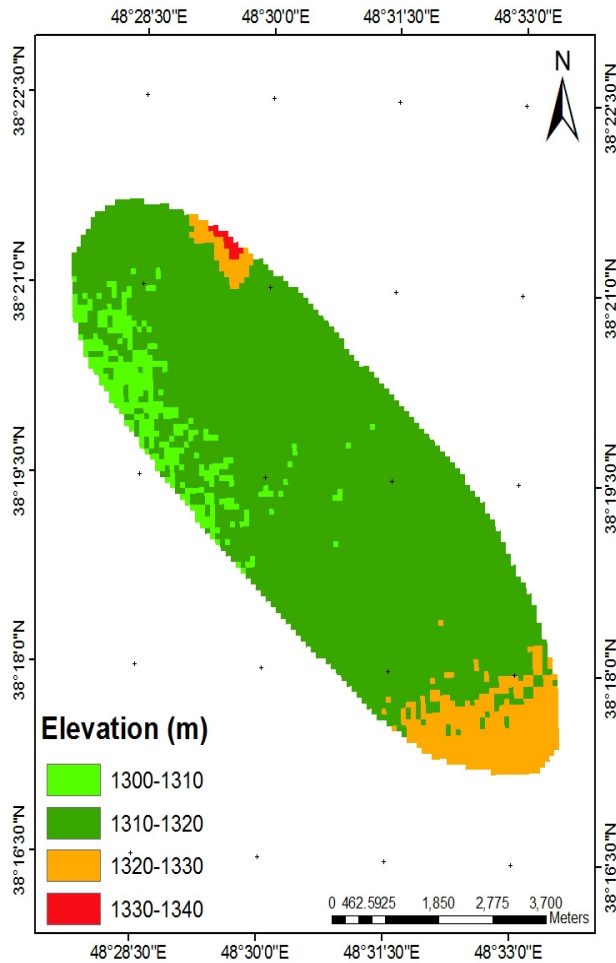


Figure 3. Elevation map of study area.

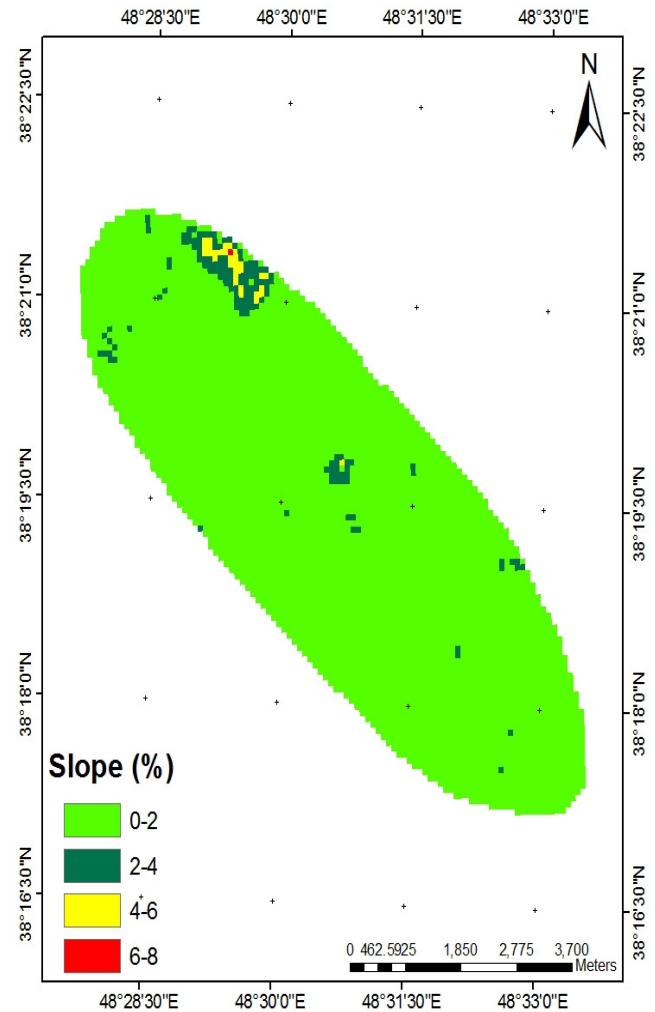


Figure 4. Slope map of study area.

areas were eliminated from the classified image.

Digital elevation model (DEM) was performed by digitizing 1/50000 scaled standard topographic map. The resultant map indicates that the study area has an altitude ranging from approximately 1300 to 1340 m above sea level. Then digital elevation model was classified to four classes with 10 m intervals and elevation map of the study area was produced. Finally, slope map was derived by using the DEM as layers in GIS and overlain on the classified image to delineate final land cover classes including slope limits of study area. Figures 3 and 4 show the elevation and slope map of the study area, respectively. As can be seen in them, the most part of the region lies at an altitude of 1310 to 1320 m and a slope of 0 to 2%.

The final land cover map is illustrated in Figure 5 showing physiographic characteristics of each land cover types. In this study, five land cover types were identified, including: Range, grass land, dry farming, irrigated farming, and urban were identified. Table 2 shows the area statistics of each class obtained from the classified image.

Table 3 shows the classified results on the top as compared with the reference data (ground truth) for the corresponding points along the left. Examination of the Irrigated farming class in Table 3 shows that 166 pixels were determined to actually be irrigated farming. The overall accuracy was calculated by correctly classified pixels in the table and dividing that by adding up all of the total pixels of that class (99%). Reliability was calculated by correctly classified pixels in the table and dividing that by adding up all of the pixels were classified as irrigated farming. A total of 219 pixels were classified as irrigated farming. Of those, 166 were correctly classified, while one was range and 52 were urban. Then the reliability was 76%. Table 4 shows the result of accuracy assessment of image classification. In this table, the average accuracy is the average of the accuracies for each class and the average reliability is the average of the reliabilities for each class. Overall accuracy is a similar average with the accuracy weighted by the proportion of test samples.

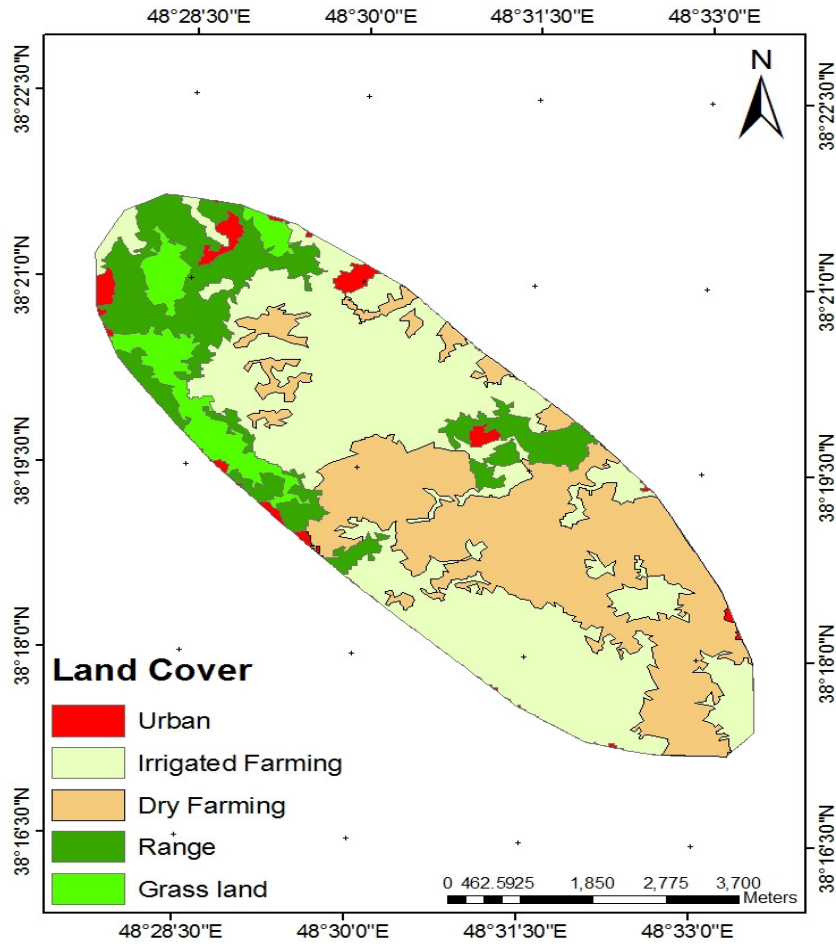


Figure 5. The final land cover map of studied area.

Table 2. Area statistics of each class.

Class	Area	Percent
Urban	119.12	3.51
Irrigated farming	1354.6	39.95
Dry farming	1119.37	33
Range	520.31	15.34
Grass land	278.14	8.2
Total	3391.54	100

Table 3. Confusion matrix of classified image.

Class	Urban	Irrigated farming	Dry farming	Range	Grass land	Accuracy
Urban	73	52	0	7	0	0.55
Irrigated farming	0	166	0	2	0	0.99
Dry farming	0	0	182	0	0	1
Range	0	1	0	40	49	0.44
Grass land	0	0	1	12	35	0.73
Reliability	1	0.76	0.99	0.66	0.42	

Table 4. Result of accuracy assessment of image classification.

Average reliability(%)	Average accuracy(%)	Overall accuracy(%)
76.50	74.29	80.00

The overall classification accuracy for the five classes was established as 80% that is sufficient for delineating of land cover in order to analyze.

Conclusions

Using remote sensing techniques to develop land use classification is a useful and detailed way to improve the selection of areas designed to agricultural, urban and/or industrial areas of a region (Selçuk, 2003). Since the remote sensing data to be used in GIS media are of raster data format, they are of limited use in certain applications. Use of vector data besides the raster data in making the analyses is needed especially in land management and land use planning studies. In this study, each class obtained by means of classifying the satellite image has been transformed into vector data and transferred to GIS media, and then, area related queries were made. Moreover image classification decreases the amount of time and effort required to generate land cover map and using GIS in combination with image analysis, users can easily define the concerning criteria to select the area and decision making process. The results showed that classification of LISS III Imagery to produce land cover map has a high overall accuracy. In this area, there was no digital land cover map and using this procedure, the land cover map was generated. more to the point the ancillary data such as slope and elevation information of each class is added to the classified image and map overlaying technique was applied to describe the quantitative relationships among land cover classes, slope and elevation criteria. As a result, land cover map of the Ardebil showed in Figure 3 was produced. Therefore this map could be useful for subsequent applications such as land use planning.

REFERENCES

- Anderson AB, Wang G, Gertner G (2006). Local variability based sampling for mapping a soil erosion cover factor by co-simulation with Landsat TM images. *Int. J. Remote Sensing*, 27: 2423-2447.
- Berberoglu S, Evrendilek F, Ozkan C, Donmez C (2007). Modeling forest productivity using Envisat MERIS data. *Sensors*, 7: 2115-2127.
- Chavez PSJ (1988). An improved dark object subtraction technique for atmospheric correction of multispectral data. *Remote Sensing Environ.*, 24: 459-479.
- De Jong BHJ (1999). Land use change and carbon flux between 1970s and 1990s in Central Highlands of Chiapas, Mexico. *Environ. Manage.*, 23: 373-385.
- Ehlers M, Jadkowski MA, Howard RR, Brousten DE (1990). Application of SPOT data for regional growth analysis and local planning. *Photogramm. Eng. Remote Sensing*, 56: 175-180.
- Evrendilek F (2007). Integrating map algebra and statistical modeling for spatio-temporal analysis of monthly mean daily incident photosynthetically active radiation (PAR) over a complex terrain. *Sensors*, 7: 3242-3257.
- Evrendilek F, Berberoglu S, Gulbeyaz O, Ertekin, C (2007). Modeling potential distribution and carbon dynamics of natural terrestrial ecosystems: A Case Study of Turkey. *Sensors*, 7: 2273-2296.
- Gupta RP (2003). *Remote Sensing Geology*, 2nd Edition (Heidelberg: Springer-Verlag).
- Gupta RP, Saha AK, Arora, MK, Kumar A (1999). Landslide hazard zonation in a part of the Bhagirathi Valley, Garhwal Himalayas, using integrated remote sensing -GIS. *Himalayan Geol.*, 20(2): 71-85.
- Harris PM, Ventura SJ (1995). The integration of geographic data with remotely sensed imagery to improve classification in an urban area. *Photogramm. Eng. Remote Sensing*, 61: 993-998.
- Hirataa M, Kogab N, Shinjoc H, Fujitad H, Gintzburger G, Miyazaki A (2001). Vegetation classification by satellite image processing in a dry area of northeastern Syria. *Int. J. Remote Sensing*, 22: 507-516.
- Janssen LF, Vander WJ (1994). Accuracy: a Review. *Photogramm. Eng. Remote Sensing*, pp. 419-425.
- Jensen JR (1986). *Introductory Digital Image Processing: A Remote Sensing Perspective*: New Jersey, Prentice-Hall.
- Jensen JR (1996). Merging different types of remotely sensed data for effective visual display. *Introductory Digital Image Processing: A Remote Sensing Perspective*, 2nd ed: Prentice-Hall, Upper Saddle River, NJ.
- Saha AK, Gupta RP, Arora MK (2002). GIS-based landslide hazard zonation in the Bhagirathi (Ganga) Valley, Himalayas. *Int. J. Remote Sensing*, 23(2): 357-369.
- Selçuk R, Nişancı R, Uzun B, Yalçın A, Inan H, Yomralioğlu T (2003). Monitoring land -use changes by GIS and remote sensing techniques: Case Study of Trabzon. 2nd FIG Regional Conference, Urban-Rural Interrelationship for Sustainable Environment, Marrakech, Morocco.
- Shi PJ, Yuan Y, Zheng J, Wang JA, Ge Y, Qiu GY (2007). The effect of land use/cover change on surface runoff in Shenzhen region, China. *Catena*, 69: 31-35.
- Vieira IGC, De Almeida AS, Davidson EA, Stone TA, De Ccarvalho CJR, Guerrero JB (2003). Classifying successional forests using Landsat spectral properties and ecological characteristics in eastern Amazonia. *Remote Sensing of Environ.*, 87: 470-481.
- Weng Q (2001). A remote sensing - GIS evaluation of urban expansion and its impact on surface temperature in the Zhujiang Delta, southern China. *Int. J. Urban Regional Stud.*, 22: 425-442.
- Xiaoling C, Xiaobin C, Hui L (2006). Expert classification method based on patch-based neighborhood searching algorithm. *Geo-Spatial Info. Sci.*, 1 10(1): 37-43.
- Zhu AX (1997). Measuring uncertainty in class assignment for natural resource maps under fuzzy logic. *Photogramm. Eng. Remote Sensing*, 63 (10): 1195-1202.